Influence of internal curing admixture on hardening process of mortars with ground granulated blast-furnace slag (GGBS)

Do Couto Rosa Almeida, Fernando ; Klemm, Agnieszka

Published in:
Proceedings of the 1st International ICT Conference on Cement and Concrete Technology

Publication date:
2017

Document Version
Publisher's PDF, also known as Version of record

1st International Conference on Cement & Concrete Technology
Muscat, Sultanate of Oman
20-22 Nov 2017
www.concreteconference.org.uk

Influence of internal curing admixture on hardening process of mortars with ground granulated blast-furnace slag (GGBS)

F.C.R. Almeida & A.J. Klemm
School of Engineering and Built Environment, Glasgow Caledonian University, Glasgow, UK

ABSTRACT: Superabsorbent polymers (SAP) can be used as internal curing agent in order to control self-desiccation process in cementitious materials. This paper aims to evaluate the influence of SAPs on hardening process of PC-GGBS mortars. Different mortars combinations modified by GGBS and SAPs have been considered. Autogenous shrinkage, microstructural characteristics (MIP/SEM) and mechanical properties have been analyzed at 7, 14 and 28 days. The results showed that both studied SAPs can reduce autogenous shrinkage for all GGBS contents. In particular SAP with low water absorption capacity can even lead to prior expansion of mortars, in particular for lower GGBS contents. It confirms that kinetics of SAP sorption plays a critical role in the hardening process. Although it increases total porosity, SAP addition can decrease pore sizes and reduce pores interconnectivity. Therefore, the type of SAP strongly influences progress of curing process, especially when different GGBS concentrations are considered.

1 INTRODUCTION

The increase of concrete durability is a constant concern among researchers and practitioners in Construction Industry. The challenge is to produce more and more durable cementitious materials in order to increase building lifespan, conserve natural resources and reduce wastes generated from repair and replacement services. One of the most serious problems regarding reduction of concrete durability is related to microstructural development during hardening process. The propagation of microcracks establishes interconnections and increases permeability of the system. Thus, the presence of a well interconnected network of macro and microcracks can facilitate concrete exposure to several physical and chemical deterioration processes (Bertolini et al 2013, Ribeiro et al 2013, Mehta & Monteiro 2005).

In general, for concrete based on ordinary Portland cement (PC), coefficient of permeability is exponentially reduced when the fractional volume of capillary pores is decreased by hydration process. Although there is a considerable increment in pores volume due to C-S-H interlayer space and small capillaries, the permeability is greatly reduced with increasing degree of hydration. Thus, permeability is directly related to the volume of larges pores, usually bigger than about 100 nm (Mehta & Monteiro 2005). This is probably because pore systems that comprise mainly small

pores tend to be more discontinuous and not well interconnected. Therefore, the higher amount of smaller pores the lesser is permeability and hence the interconnectivity of the hardened concrete network.

Addition of supplementary cementitious materials usually leads to higher total porosity than a PC system due to the decrease in total volume of hydrates formed. However, blended cements can produce a more refined pore structure (Scrivener et al 2015, Lothenbach et al 2011, Loser et al 2010, Ouellet et al 2007). In particular, mixes with ground granulated blast-furnace slag (GGBS) may contain more fine pores and less coarse capillary pores than a PC paste, resulting in a reduced permeability (Lothenbach et al 2011).

This refinement of capillary pores by GGBS, however, can also lead to another undesired effect: increase in autogenous shrinkage (Almeida & Klemm 2016a, Valcuende et al 2015, Bouasker et al 2014, Jiang et al 2014, Lee et al 2006). This shrinkage trigged by self-desiccation processes may lead to cracking formation and hence opening of cementitious matrix microstructure, resulting in an opposite effect of increased permeability. In this context, superabsorbent polymers (SAP) can be used as internal curing agent in order to control self-desiccation process in cementitious materials (Klemm et al 2016, Snoeck et al 2015, Beushausen el al 2014, Mechtcherine et al 2013, Mechtcherine & Reinhardt 2012). Its high ability to instantaneously absorb water from fresh mix (Figure 1) and release this water during hydration processes may suggest SAP application in controlling cracking susceptibility, reducing permeability and hence

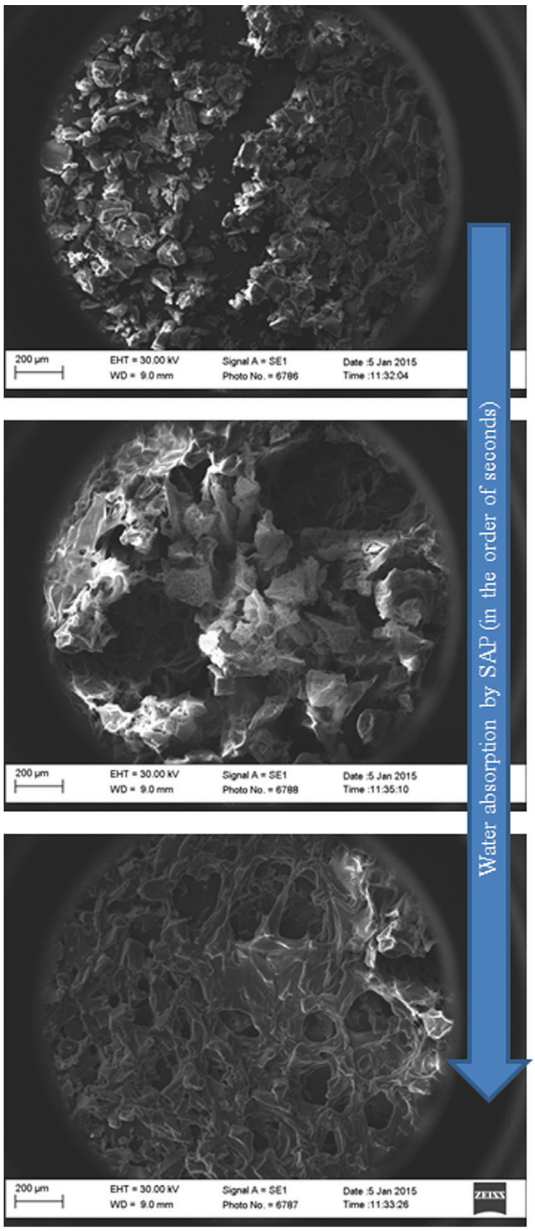

Figure 1. Evolution of SAP water absorption over the time (in the order of seconds): from dry to gel formation.

contributing for enhanced concrete durability (Beushausen et al 2014, Zhutovsky & Kovler 2012).

Therefore, this paper aims to evaluate the effect of SAPs as internal curing admixture on hardening process of PC-GGBS mortars. Autogenous shrinkage, microstructural features and mechanical properties have been analyzed in order to understand the effects on their pore sizes and pores interconnectivity.

2 METHODOLOGY

Different mortar compositions have been considered in the experimental programme; four levels of Portland cement (CEM I 52.5N) replacement by GGBS (0%, 25%, 50% and 75%) were adopted. Chemical analysis of CEM I and GGBS are presented in Table 1 and are in accordance with BS EN 197-1 (2011) and BS EN 15167-1 (2006), respectively.

Table 1. Chemical composition (%) of CEM I and GGBS.

Compound (%)	CEM I	GGBS	Compound (%)	CEM I	GGBS
SiO_2	20.07	34.53	Na_2O	0.31	0.17
Al_2O_3	4.85	13.14	K_2O	0.62	0.59
Fe_2O_3	2.72	0.21	Cl	0.06	0.02
CaO	62.44	38.53	MnO	-	0.22
MgO	2.20	9.74	TiO_2	-	0.82
SO_3	3.15	0.35	LOL	2.77	0.64

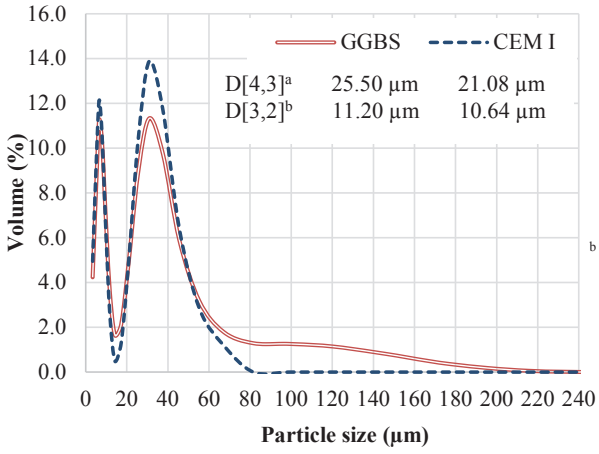

Figure 2. Particle size distribution for CEM I and GGBS.

[a] D[4,3] = main equivalent diameter (volume)
[b] D[3,2] = main equivalent diameter (surface area)

Analysis of particle size distribution by using a Laser Difractometry Xmastersize (air as dispersant) showed that GGBS comprises larger particles than CEM I (Figure 2). While GGBS contained 90% of particles distributed below 49.78 µm, CEM I had the same amount distributed under 41.55 µm.

Two types of SAPs with different water absorption capacities (SAP-10 = 10g/g and SAP-25 = 25-30g/g in cement paste solution) have been considered as internal curing admixtures. Both SAPs had particles with sizes in the range of 63-125 μm. The adopted SAP content was 0.25% by mass of binder.

Mortars have been prepared in the proportion of 1:2 (binder: fine sand) and with water/binder ratio (w/b) of 0.5. Table 2 shows the mortar samples analyzed in this paper.

Table 2. Mortars samples used in the experimental programme.

Sample	Type of SAP	CEM I (%)	GGBS (%)
R0	-	100	0
R25		75	25
R50		50	50
R75		25	75
X0	SAP-25	100	0
X25		75	25
X50		50	50
X75		25	75
Z0	SAP-10	100	0
Z25		75	25
Z50		50	50
Z75		25	75

In order to analyze the effect of SAPs on self-desiccation of GGBS-PC mortars, autogenous shrinkage has been evaluated by sealed corrugated tubes method during the first 28 days (ASTM C-1698, 2009). Measurements started from the final set time and were taken at least twice every day using a digital bench dilatometer. Average of three samples was considered.

The influence of internal curing by SAPs was also investigated by analyzing microstructural characteristics and mechanical properties at 7, 14 and 28 days. Mortars were molded into prismatic specimens (160 x 40 x 40 mm), demolded after 48 hours and then stored in climatic chamber (T = 21 ± 2 ºC and RH = 40 ± 5%) until the age of testing.

Microstructural features including total intrusion volume (mL/g), total extrusion volume (mL/g), total pore area[1] (m^2/g), total porosity (%) and intrusion-extrusion hysteresis were obtained by the Mercury Intrusion Porosimetry (MIP) technique. Interconnectivity and shape of pores of SAP mortars were verified by %Hg retained into samples (intrusion/extrusion ratio) and compared to their respective reference samples. Pore sizes were analysed by surface area/volume ratio (SA/V). This last parameter was calculated in order to compare different sizes of pores per unit volume, it means considering all pores to the same level of total intrusion volume (total porosity). Scanning Electron Microscopy (SEM) technique was also considered to evaluate pores characteristics.

1 Pore surface area is obtained as $\Sigma\Delta A=-(\Sigma P\Delta V)/\gamma\cos\theta$, where γ is the surface tension of mercury and θ its contact angle with the sample.

Mechanical properties were verified by standard flexural and compressive strength tests according to BS EN 1015-11 (1999). Average of three and six samples was considered for flexural and compressive strength analysis respectively.

3 RESULTS AND DISCUSSION

Figure 3 shows results of autogenous shrinkage during the first 28 days for all GGBS contents studied. Overall, reference samples had the highest levels of shrinkage, followed by mortars with SAP-25 (X group) and mortars with SAP-10 (Z group).

Reference samples (without SAPs) presented a continuous downwards slope during the first month, leading to the greatest autogenous shrinkage values. Moreover, the greater PC replacement level the higher was autogenous shrinkage; values about -400, -500, -600 and -700µm/m have been reached at 28 days for GGBS levels of 0%, 25%, 50% and 75% respectively. This higher shrinkage can be attributed to the ability of GGBS to produce more fine pores and less coarse capillary pores than PC mortars. GGBS can act as a very fine aggregate, since its reaction rate is lower than CEM I and the use of supplementary cementitious materials decrease the total volume of hydrates formed in mortars (Valcuende et al 2015, Lothenbach et al 2011). Thus, GGBS can reduce capillaries left by fine sand and increase autogenous shrinkage.

When both SAPs are added into the mix, the levels of autogenous shrinkage are notably reduced. It shows the efficiency of those polymers in acting as an internal curing agent by

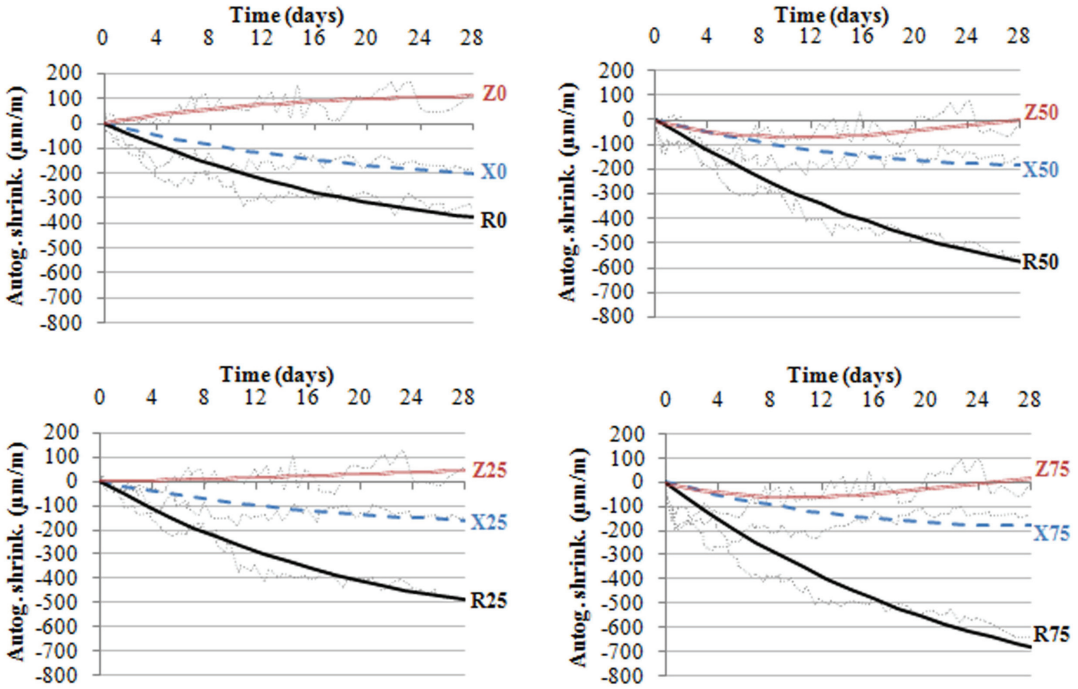

Figure 3. Autogenous shrinkage during the first 28 days (separated by GGBS content).

supplying water to help binder hydration and mitigate self-desiccation processes. SAP-25 (X group) seems to stabilize its level of autogenous shrinkage at -200μm/m for all GGBS contents at 28 days. This represents a reduction varying from 50 to 70% compared to the reference samples, for low and high GGBS content respectively. SAP-10 (Z group) in turn shows a different behaviour depending on the amount of GGBS. For low GGBS contents, this polymer leads to the relative expansion of mortar, instead of shrinkage as expected. Its low water absorption capacity does not have the ability to sustain water supply for long, and hence releases it faster than SAP-25. Thus, this expansion can be attributed to the re-absorption of bleeding water in the mixture. Alternatively, it may result from crystallization pressure of calcium hydroxide formed in the first week trigged by an increase of portlandite oversaturation (Snoeck et al 2015, Sant et al 2011). As GGBS content is increased (more than 50%), a kind of balance between SAP's expansion and GGBS's shrinkage starts to appear. Mortars can experience some slight shrinkage (below -100μm/m) during the first week followed by a relative expansion due to formation of later GGBS products.

This difference in SAPs behavior and their effects on PC-GGBS mortars can also be verified in terms of porosity and permeability. Figure 4 shows intrusion-extrusion hysteresis by MIP for GGBS-PC mortars modified by SAPs at 7, 14 and 28 days. Due to space limitations and comprehension easiness, only results for 0% and 75% of GGBS have been showed (samples with 25% and 50% of GGBS have presented intermediate behavior).

Overall, all reference curves (without SAP) show the lowest total intrusion volumes, indicating that SAPs increase total porosity of mortars. This increment in porosity is related to SAP swelling ability and turning into gel as soon as they get in contact with water from fresh mix. This increased porosity by SAP may also contribute for autogenous shrinkage mitigation by creating internal micro voids that release capillaries tensions responsible for self-desiccation processes. The increment in total porosity is also verified by increasing GGBS content in the same group of mortar (Almeida & Klemm 2016b, Lothenbach et al 2011). This is because blended cements decrease total volume of hydrates formed and, in particular, GGBS can have lower hydration rate due to larger particles sizes (Figure 1) in comparison with CEM I.

Mortars without GGBS modified by both SAPs had similar performance up to the 14th day, showing a cumulative intrusion around 0.10 mL/g (against 0.08 mL/g for the reference samples). At 28 days, mortar with SAP-25 (X0-28d) has a lower volume of total Hg intruded when compared with SAP-10 mortar (Z0-28d). This may be related to the higher water absorption capacity of SAP-25 which enables longer hydration process and hence decreases its total porosity. However, both SAPs curves seem to approach reference curve during the first month (moving from the left to the right), indicating that SAPs are able to reduce their pore sizes even with higher total porosity.

For high GGBS content, mortars with SAP-10 allow the greatest total Hg intrusion, while samples with SAP-25 seems to have similar intrusion curves when compared with the reference ones (although total porosity is higher for SAP-25). Even that, total porosity has decreased for all samples over the time.

In both cases (0% and 75% of GGBS), SAP-10 (Z group) has a tendency to increase total porosity when compared to other samples. This can be directly related to autogenous shrinkage

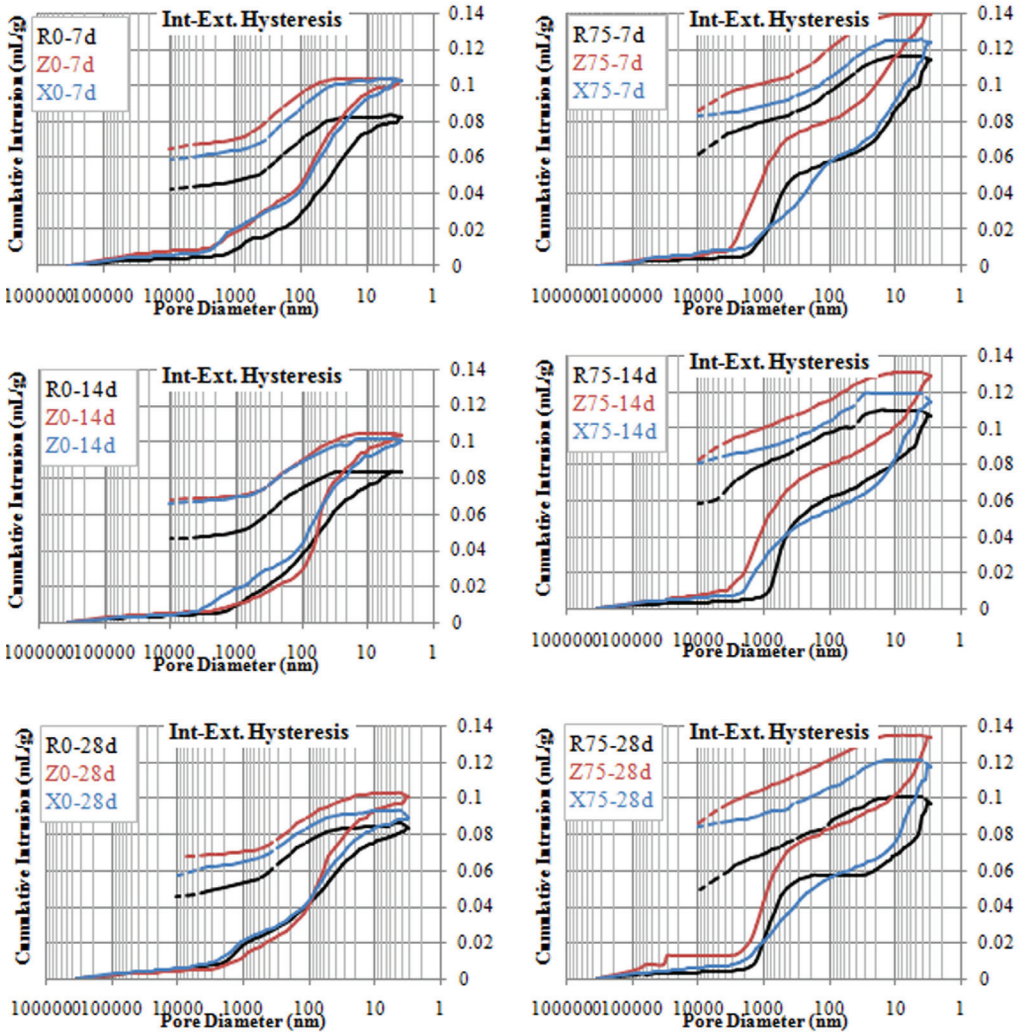

Figure 4. Intrusion-extrusion hysteresis by MIP for samples with 0% (left) and 75% (right) of GGBS at 7 (top), 14 (middle) and 28 (bottom) days.

performance (Figure 3). SAP-10 swells up into the fresh mix and helps CEM I hydration during the first hours (as it seems to have a faster water release), provoking a slight expansion (or a tendency to expansion) of mortars. Bleeding water can also be re-absorbed by SAP-10 to contribute for its mortar expansion. In the hardened state, pores are left behind which can be filled with greater difficulty by hydrated products induced by SAP (since the SAP water is gone). Total porosity for mortars without GGBS seems to be unchanged during the first 28 days. For high GGBS content mortars, later hydrated products (after the first week) can be formed by slower process of GGBS hydration, leading to slightly decreased porosity and relative expansion of Z-75 samples.

The same analysis can be done for mortars with SAP-25. The reduced total Hg intrusion for both GGBS contents over the time can justify a certain stabilization of shrinkage at 28 days for X mortars. This polymer has more ability to fill its pores with hydration products.

Another fact that can be observed from intrusion-extrusion hysteresis is the amount of mercury trapped in the sample, indicating shape and connectivity of pores. All samples showed a significant gap between both curves (intrusion and extrusion), leading to the conclusion that a considerable amount of mercury is still in the pore system after complete depressurization. Thus, pores can be considered as of low connectivity, such as closed or "ink-bottle" shape (Ma 2014, Klemm & Sikora 2013, Giesche 2006).

The shape of pores can be assumed by comparing the tendency of extrusion curves. Mortars without GGBS seem to have low slope gradient at the end of extrusion curves (above 1 μm), compared to those samples with 75% of GGBS. This steadier pattern may indicate that even with considerable pressure diminution no Hg (or low amount of Hg) is extracted from the sample. In this case, pores can be considered almost closed or with very narrow openings. On the other hand, mortars with high GGBS content have greater negative slope gradients indicating that higher amount of Hg is removed by pressure reduction. This greater ability of mercury removal can be related to the presence of pores with wider openings or with higher level of connectivity trigged mainly by micro cracking formation; the higher GGBS content the greater is autogenous shrinkage (Figure 3). The lower water absorption capacity and potential re-absorption of bleeding water by SAP-10 (due to expansion in autogenous shrinkage) may open internal micropores, leading to creation of microstructure more similar to the reference sample (both extrusion curves have higher gradients compared to SAP-25 above 1 μm). Therefore, mortars with 75% of GGBS modified by SAP-25 (group X) have the lowest slope gradient, suggesting that this polymer can have better efficiency in clogging its own pores and reducing connectivity.

The level of connectivity of pores is verified in Table 3: Column D shows %Hg retained into each sample (extrusion/intrusion) and Column E presents the relative increment of %Hg retained in comparison with reference sample (SAP extrusion/reference extrusion).

All mortars modified by SAP were able to retain more mercury than their respective reference samples. This is because SAP can facilitate a decrease in interconnectivity between pores (even with increased porosity), most likely due to its autogenous shrinkage reduction (Figure 3). It is important to stress that the greatest relative Hg retention was observed in mortar X75 (SAP-25 with 75% of GGBS), indicating that the SAP with higher water absorption capacity was able to contribute for further GGBS hydration, decreasing even more its pores connectivity.

Relative pore sizes can be analyzed by Table 4; given total intrusion volume (total pore volume, V, Column B- Table 3) and total pore surface area (SV), their relation (SA/V_{ref}) for SAP mortars in comparison with their respective reference samples are presented in Column H.

The analysis was made according to Figure 5, assuming pores with spherical shapes. Considering the same unit volume (it means regardless the difference in total porosity), positive relative SA/V_{ref} values indicate that mortar has smaller predominant pores than its respective reference sample; negative values, larger predominant pores.

Table 3. Hg intrusion-extrusion features.

Mortar	7 days					14 days					28 days				
	(A)	(B)	(C)	(D)	(E)	(A)	(B)	(C)	(D)	(E)	(A)	(B)	(C)	(D)	(E)
R0	16.43	0.082	0.042	51%	-	16.80	0.082	0.046	56%	-	16.76	0.083	0.045	55%	-
R25	18.13	0.089	0.045	51%	-	19.50	0.097	0.050	52%	-	19.66	0.099	0.064	65%	-
R50	21.83	0.111	0.055	50%	-	20.05	0.100	0.050	50%	-	17.64	0.088	0.047	54%	-
R75	21.80	0.110	0.061	56%	-	21.19	0.107	0.058	54%	-	18.93	0.097	0.058	60%	-
X0	20.12	0.100	0.058	59%	14%	19.94	0.100	0.065	65%	17%	17.60	0.089	0.057	64%	18%
X25	19.77	0.100	0.062	62%	22%	20.81	0.105	0.065	62%	20%	19.03	0.097	0.067	69%	6%
X50	22.65	0.119	0.071	60%	20%	21.74	0.113	0.073	65%	29%	21.58	0.113	0.077	68%	26%
X75	22.33	0.115	0.082	72%	28%	21.88	0.114	0.080	70%	30%	20.33	0.105	0.084	80%	35%
Z0	19.96	0.102	0.065	64%	24%	19.91	0.101	0.067	67%	20%	19.74	0.100	0.067	67%	23%
Z25	21.79	0.113	0.071	63%	24%	21.81	0.114	0.073	64%	23%	21.02	0.109	0.076	70%	8%
Z50	25.08	0.133	0.082	61%	22%	22.06	0.114	0.068	60%	19%	23.32	0.123	0.079	64%	19%
Z75	26.03	0.138	0.085	62%	10%	23.22	0.124	0.082	67%	23%	25.39	0.133	0.086	65%	8%

(A) Total porosity (%)
(B) Total intrusion volume (mL/g)
(C) Total extrusion volume (mL/g)
(D) %Hg Retained (Extr/Intr) – Column (C)/ Column (B)
(E) Relative %Hg Retained to its respective Reference sample – SAP Column (C) / Ref Column (C)

Table 4. Relative pore sizes by MIP.

Mortar	7 days			14 days			28 days		
	(F) T.P Area	(G) SA/V ratio	(H) Relative SA/V_{ref}	(F) T.P Area	(G) SA/V ratio	(H) Relative SA/V_{ref}	(F) T.P Area	(G) SA/V ratio	(H) Relative SA/V_{ref}
R0	13.223	160.67	-	10.085	121.95	-	10.746	129.16	
R25	15.028	168.76	-	14.852	152.48	-	9.182	92.00	
R50	18.840	169.35	-	22.662	224.60	-	11.272	127.80	
R75	24.518	221.89	-	25.238	235.43	-	27.780	285.51	
X0	13.429	134.36	-16%	13.561	134.80	11%	9.959	111.40	-14%
X25	12.958	128.42	-24%	18.378	174.20	14%	12.678	130.16	41%
X50	18.286	153.02	-10%	16.267	143.83	-36%	16.406	144.55	13%
X75	29.436	255.64	15%	27.725	242.14	3%	32.939	313.11	10%
Z0	12.275	119.87	-25%	14.250	140.19	15%	13.143	130.39	1%
Z25	13.479	119.28	-29%	16.615	145.24	-5%	15.638	143.47	56%
Z50	18.739	139.95	-17%	18.490	161.77	-28%	21.041	170.23	33%
Z75	24.253	174.61	-21%	27.055	218.10	-7%	29.826	223.25	-22%

Total pore area (m^2/g)
SA/V ratio is the relation between total pore area (m^2/g) and total intrusion volume (mL/g). It indicates pore surface area per unit volume. Column (F)/ Column (B), Table 3.
Relative SA/V_{ref} is a comparative of SA/V ratio (Column H) in relation to its respective reference samples: negative values indicate larger pores than those for reference samples; positive values, smaller pores.

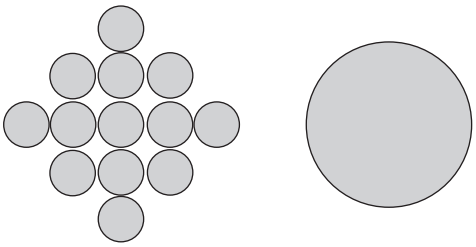

Total volume	=	Total volume
Total surface area	>	Total surface area
SA/V ratio	>	SA/V ratio

[Left] Figure 5. Comparative representation between two set of pores: different predominant sizes but with the same total volume.

[Below] Figure 6. SEM micrographs of mortars modified by SAP at 7 (left) and 28 (right) days. Collapsed SAP Z into the hardened mortar is highlighted for one week mortar.

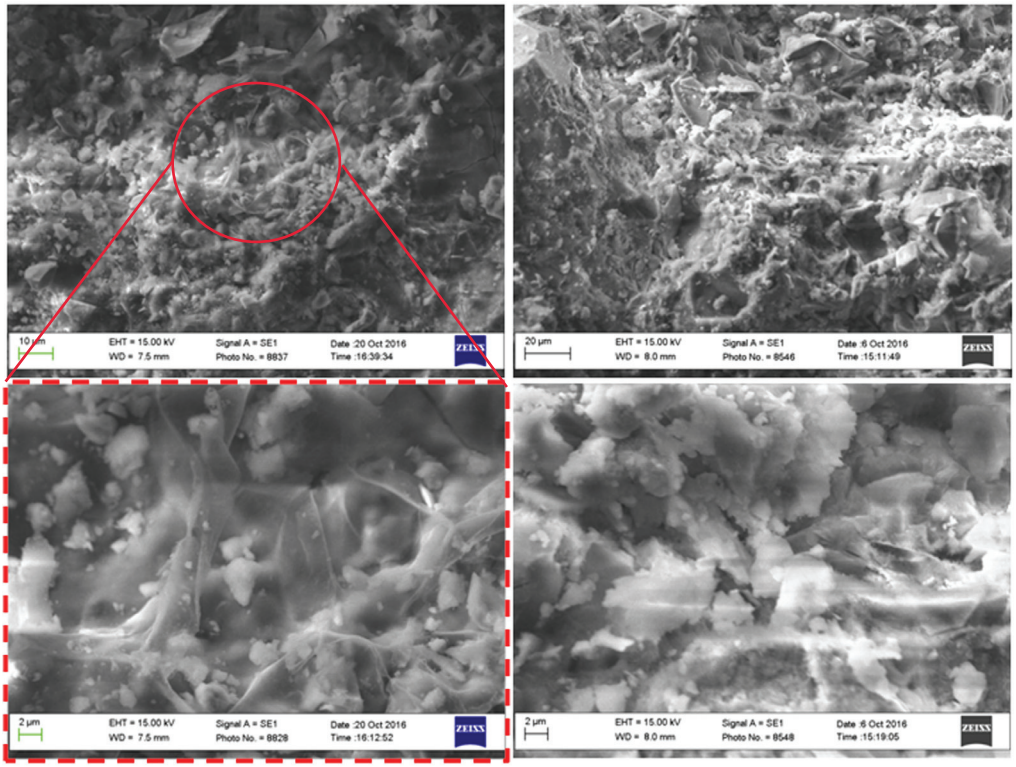

Overall, most of mortars modified by SAP presented larger pores than its respective reference sample at 7 days. In early ages, SAP pores are formed due to its initial swelling and gel formation from fresh mix (water contact). However, with the passage of time, hydrated products fill these voids, reducing the size of larger pores and/or decreasing connectivity between them. Thus, the majority of SAP samples show positive values of SA/V_{ref} at 28 days; SAP can help hydration reactions by changing its microstructure and hence being able to produce more resistant mortars to eventual aggressive agents attack and degradation processes. Therefore,

although SAPs produce larger pores in the first week, these pores are able to fill themselves and turn into smaller pores at 28 days (even with higher total porosity). This reduction in pore size over time is aligned with hysteresis curves analysis in particular for PC mortars modified by SAPs (Figure 4).

Indeed, SEM micrographs show this microstructure evolution of SAP samples between 7 and 28 days (Figure 6). At the first week, collapsed SAP gel can be observed in the hardened sample; it was big enough to be noted by the SEM technique. However, at the end of four weeks, it was not possible to identify any SAP residue (vestige) for any sample, assuming that SAP pores have been filled mainly by C-S-H and $Ca(OH)_2$.

Predominance of smaller pores at 28 days reflects directly on flexural strength results (Figure 7). Overall, mortars with SAPs showed lower values (difference of up to 10% at 28 days) of flexural strength compared to their respective reference samples. Reduction in flexural strength by SAPs was also noted by other authors (Mechtcherine et al 2013, Beushausen et al 2014). Moreover, the higher GGBS content the lower flexural strength. This can be attributed to larger particles of GGBS (Figure 2) and lower hydration rate when compared to CEM I. This pattern was observed in all groups of mortars at all ages. GGBS reactivity decreases with decreasing pH due to smaller amount of PC in the blended mix (Lothenbach et al 2011, Taylor et al 2010).

Figure 8 shows results of compressive strength at 7, 14 and 28 days. Values for SAP mortars are very comparable to the reference samples, especially after four weeks of internal curing. Although higher total porosity, SAPs was able to change mortar microstructure from larger pores (at the first week) to a very non-interconnected network of smaller pores at 28 days. Even with some reductions at 7 days, compressive strength results for SAP samples were similar to those for mortars without SAP at the same level of GGBS. When GGBS content is increased, the same pattern for flexural strength is attained: compressive strength is reduced by the increment of GGBS for all groups of mortars.

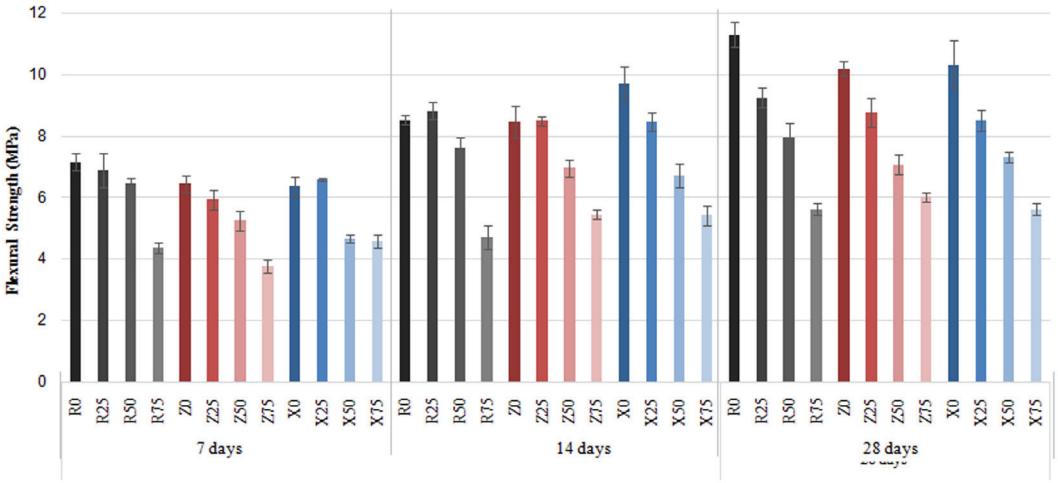

Figure 7. Results of flexural strength at 7, 14 and 28 days.

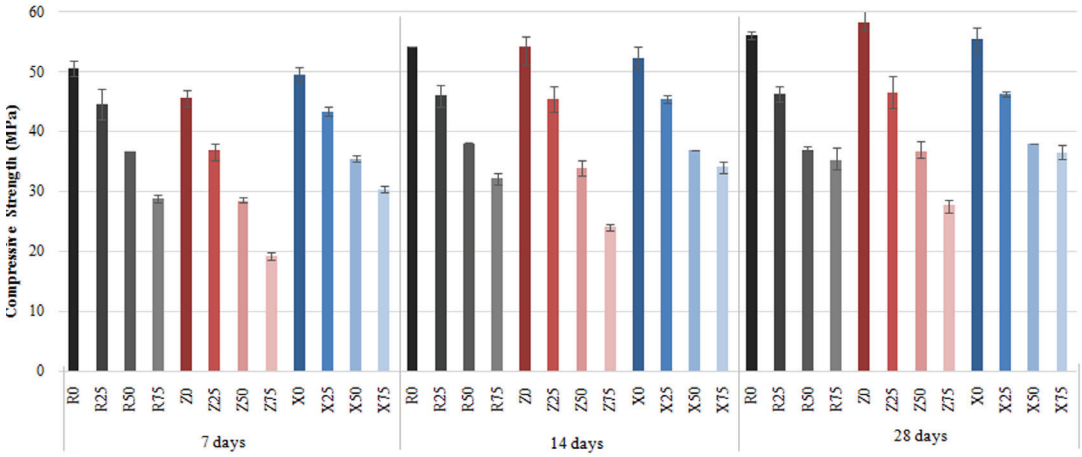

Figure 8. Results of compressive strength at 7, 14 and 28 days.

Therefore, mechanical properties are directly affected by increasing of GGBS. Although SAPs have slightly reduced overall flexural strength at 28 days, compressive strength is kept in the same order of the respective reference sample.

4 CONCLUSIONS

From the results obtained in the experimental study, the following can be concluded:

- Autogenous shrinkage of PC-GGBS mortars can be significantly reduced by addition of SAPs as internal curing admixture. SAP-25, with higher water absorption, is able to reduce autogenous shrinkage by about 50-70% in relation to the reference samples at 28 days. SAP-10 may have a faster water desorption leading to mortar expansion for low GGBS contents due to the crystallization pressure of calcium hydroxide or a potential ability of this polymer to re-absorb bleeding water from the mixture. For higher GGBS contents, a relative expansion is achieved after the first week due to later hydration of GGBS products;
- Although internal curing agents may lead to increased total porosity, SAPs can decrease pore sizes and reduce pores interconnectivity of PC-GGBS mortars compared to the reference samples. Mortars with 75% of GGBS modified by SAP-25 have the best efficiency in clogging its own pores and reducing connectivity during the first month compared to the other samples. Reduction in voids interconnectivity suggests more durable cementitious materials since they are less prone to suffer from physical and chemical deterioration processes;
- The formation of smaller pores by SAP addition leads to slight reduction in flexural strength (less than 10%) of PC-GGBS mortars at 28 days. However, compressive strength values of SAP mortars are almost unaffected.

ACKNOWLEDGEMENTS

The authors acknowledge CNPq (Conselho Nacional de Desenvolvimento Científico e Tecnológico – Brazil) for the financial support, BASF for SAPs supply and Dr Andrew Cowell for Laser Difractometry analysis support.

REFERENCES

Almeida, F.C.R. & Klemm, A.J. (2016a). Effect of superabsorbent polymers (SAP) on fresh state mortars with ground granulated blast-furnace slag (GGBS). In: *5th International Conference on Durability of Concrete Structures, Proc*., Shenzhen, 2016.

Almeida, F.C.R. & Klemm, A.J. (2016b). Evaluation of hardened state properties of GGBS-PC mortars modified by superabsorbent polymers (SAP). In: *International RILEM Conference on Materials, Systems and Structures in Civil Engineering, Proc.*, Lyngby, 2016.

ASTM C-1698. (2009). Standard test method for autogenous strain of cement paste and mortar. American Society for Testing and Materials, USA.

Bertolini, L.; Elsener, B.; Pedeferri, P.; Redaelli, E.; Polder, R.B. (2013). *Corrosion of steel in concrete: prevention, diagnosis, repair.* 2ed. Wiley-VCH.

Beushausen, H.; Gillmer, M.; Alexander, M. (2014). The influence of superabsorbent polymers on strength and durability properties of blended cement mortars. *Cement and Concrete Composite* Vol. 52, 73–80.

Bouasker, M.; Khalifa, N.H.; Mounanga, P.; Kahla, N.B. (2014). Early-age deformation and autogenous cracking risk of slag–limestone filler-cement blended binders. *Construction and Building Materials* Vol. 55, 158–167.

BS EN 197-1. (2011). Cement – Part 1: Composition, specifications and conformity criteria for common cements. BSI.

BS EN 1015-11. (1999). Methods of test for mortar for masonry – part 11: Determination of flexural and compressive strength of hardened mortar. BSI.

BS EN 15167-1. (2006). Ground granulated blast furnace slag for use in concrete, mortar and grout. Definitions, specifications and conformity criteria. BSI.

Giesche, H. (2006). Mercury Porosimetry: a general (practical) overview, *Part Part Syst Charact* Vol. 23, 9-19.

Jiang, C.; Yang, Y.; Wang, Y.; Zhou, Y.; Ma, C. (2014). Autogenous shrinkage of high performance concrete containing mineral admixtures under different curing temperatures. *Construction and Building Materials* Vol. 61, 260–269.

Klemm, A.J.; Almeida, F.C.R.; Sikora, K.S. (2016). Application of superabsorbent polymers (SAP) in cementitious materials with blended cements. *Concrete Plant International Journal* Vol. 4, 50-58.

Klemm, A.J.; Sikora, K.S. (2013). The effect of Superabsorbent Polymers (SAP) on microstructure and mechanical properties of fly ash cementitious mortars. *Construction and Building Materials* Vol. 49, 134–143.

Lee, K.M.; Lee, H.K.; Lee, S.H.; Kim, G.Y. (2006). Autogenous shrinkage of concrete containing granulated blast-furnace slag. *Cement and Concrete Research* Vol. 36(7), 1279–1285.

Loser, R.; Lothenbach, B.; Leemann, A.; Tuchscnmid, M. (2010). Chloride resistance of concrete and its binding capacity: comparison between experimental results and thermodynamic modeling, *Cement and Concrete Composites* Vol. 32(1), 34–42.

Lothenbach, B.; Scrivener, K.; Hooton, R.D. (2011). Supplementary cementitious materials. *Cement and Concrete Research*, Vol. 41, 1244-1256.

Ma, H. (2014). Mercury intrusion porosimetry in concrete technology: tips in measurement, pore structure parameter acquisition and application, *J Porous Mater* Vol. 21, 207–215.

Mechtcherine, V.; Reinhardt, H. W. (eds.). (2012). *Application of superabsorbent polymers (SAP) in concrete construction: state-of-the-art report prepared by Technical Committee 225-SAP*, RILEM: Springer.

Mechtcherine, V. et al. (2013). Effect of internal curing by using superabsorbent polymers (SAP) on autogenous shrinkage and other properties of a high-performance fine-grained concrete: results of a RILEM round-robin test. *Materials and Structures* Vol. 47(3), 541–562.

Mehta, P.K.; Monteiro, P.J.M. (2005). *Concrete: microstructure, properties, and materials*, 3ed., McGraw-Hill.

Ouellet, S.; Bussière, B.: Aubertin, M.; Benzaazoua, M. (2007). Microstructural evolution of cemented paste backfill: mercury intrusion porosimetry test results, *Cement and Concrete Research* Vol. 37(12), 1654–1665.

Ribeiro, D.V.; Sales, A.; Souza, C.A.C.; Almeida, F.C.R.; Cunha, M.P.T.; Lourenco, M.Z.; Helene, P.R.L. (2013). *Corrosão em estruturas de concreto armado: teoria, controle e métodos de análise.* 1ed. Rio de Janeiro: Elsevier.

Sant, G.; Lothenbach, B.; Juilland, P.; Le Saout, G.; Weiss, J.; Scrivener, K. (2011). The origin of early age expansions induced in cementitious materials containing shrinkage reducing admixtures. *Cement and Concrete Research* Vol.

41, 218–229.

Scrivener, K.L.; Juilland, P.; Monteiro, P.J.M. (2015). Advances in understanding hydration of Portland cement. *Cement and Concrete Research* Vol. 78, 38–56.

Snoeck, D.; Jensen, O.M.; De Belie, N. (2015). The influence of superabsorbent polymers on the autogenous shrinkage properties of cement pastes with supplementary cementitious materials. *Cement and Concrete Researc,* Vol. 74, 59–67.

Taylor, R.; Richardson, I.G.; Brydson, R.M.D. (2010). Composition and microstructure of 20-year-old ordinary Portland cement–ground granulated blast-furnace slag blends containing 0 to 100% slag. *Cement and Concrete Research,* Vol. 40(7), 971–983.

Valcuende, M.; Benito, M.; Parra, C.; Miñano, I. (2015). Shrinkage of self-compacting concrete made with blast furnace slag as fine aggregate. *Construction and Building Materials* Vol. 76, 1–9.

Zhutovsky, S.; Kovler, K. (2012). Effect of internal curing on durability-related properties of high performance concrete. *Cement and Concrete Researc,* Vol. 42, 20–26.